European J. of Inorganic Chemistry **2020**, 2105-2111

https://doi.org/10.1002/ejic.202000250

Diiminepyridine-Supported Phosphorus (I) and (III) Complexes: Synthesis, Characterization and Electrochemistry

*Dr. Paul A. Gray,[a] Jason D. Braun,[a] Naser Rahimi,[a] and Prof. Dr. David E. Herbert[a,]**

[a]Department of Chemistry and the Manitoba Institute for Materials, University of Manitoba, 144 Dysart Road, Winnipeg, Manitoba, R3T 2N2, Canada

*david.herbert@umanitoba.ca; https://home.cc.umanitoba.ca/~dherbert/

ABSTRACT: Diiminepyridines (DIP) are popular redox "non-innocent" ligands with widespread application in late, first-row transition metal mediated catalysis and coordination chemistry. Here, we report the isolation and characterization of a pair of phosphorus coordination complexes in the +1 and +3 oxidation states supported by the same ligand framework bearing sterically imposing and electron-releasing *t*Bu substituents on the imine carbons of the DIP backbone. Electrochemical analysis demonstrates that the DIP scaffold can retain its ability to serve as an electron reservoir when coordinated to a reduced pnictogen centre, with a reversible reduction observed for the P(I) complex.

Table of Contents Graphic

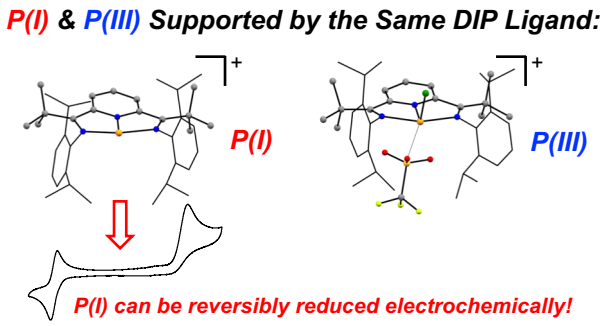

Table of Contents Entry

The synthesis of phosphorus coordination complexes of redox non-innocent diiminepyridine (DIP) ligands with the pnictogen in both P(I) and P(III) oxidation states is presented. Electrochemical characterization indicates the DIP scaffold can retain its ability to act as an electron reservoir when coordinated to main-group elements.

Key Topic Main-group coordination chemistry

Keywords main-group compounds • redox-active ligands • (diimine)pyridines (DIP)

INTRODUCTION

Diiminepyridines (DIPs, Figure 1)[1] are among the most popular redox "non-innocent" ligands,[2-4] so-called as the ligand can serve as an additional site for oxidation/reduction events in metal coordination complexes.[5] In addition to widespread application in late, first-row transition metal mediated catalysis,[6] they are also used for their simple ability to bind early transition metals,[7,8] rare earths,[9] and main-group elements in a tridentate, pincer-like fashion.[4] With respect to the p-block, DIP complexes are known for Groups 13,[10-12] 14,[13,14] 15[15-18] and 16[19,20] centres. Such complexes have found use, for example, in Lewis acid mediated catalysis including C-F bond allylation,[18] although in such scenarios, hemi-lability (chemical non-innocence) of the supporting ligands rather than redox non-innocence can be prized.[21]

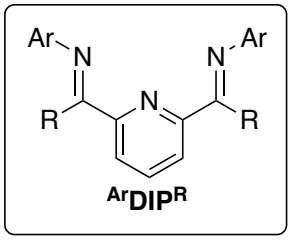

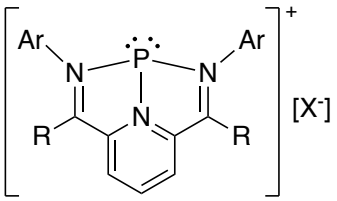

[dippDIPPhP][I3] (*ref.*[16])
[dippDIPHP][Br, I3 or B12Cl12] (*ref.*[16])
[FcDIPHP][I3] (*ref.*[17])
[dippDIPtBuP][BPh4 or OTf] (*this work)*

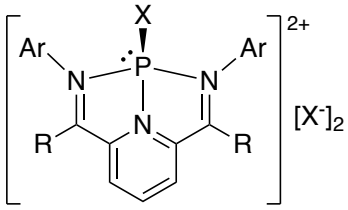

[dippDIPMePPh][OTf]2 (*ref.*[18])
[MesDIPMePPh][OTf]2 (*ref.*[18])
[dippDIPtBuPCl][OTf]2 (*this work)*

Figure 1. The diiminepyridine (DIP) scaffold, known P(I)[16,17] and P(III)[18] complexes of DIP ligands: dipp = 2,6-di(*iso*propyl)phenyl; Fc = ferrocenyl; Mes = 2,4,6-trimethylphenyl; and those described in this work.

A limited number of DIP complexes of phosphorus have been described in the literature. This includes select examples of complexes with P(I) oxidation states[16,17] and two examples of phenyl-substituted dicationic P(III) complexes.[18] In surveying known $[DIP(P)]^{n+}$ complexes, we note that

pairs of P(I) and P(III) complexes supported by the same DIP ligand scaffold have not been reported. The redox chemistry of $[DIP(P)]^{n+}$ complexes is usually discussed in the context of their preparation. For example, one route to the generation of Pn(I) (Pn = pnictogen) congeners is to take advantage of spontaneous reduction of P(III) or As(III) halides via elimination of X_2 upon coordination of a multidentate ligand.[22,23] This approach can be dependent on the nature of the chelating ligand: isolation of P(III) complexes without reductive X_2 elimination has been observed with related anionic diarylamido *P^N^P* ligands.[24] In comparison, α-diimine supported P(I) centres will spontaneously engage in electron transfer with more easily reduced α-diimine ligands, forming *N*-heterocyclic phosphenium P(III) cations supported by the resulting formally dianionic ligand.[25] With respect to any discussion of the redox behavior of isolated DIP(P) complexes, the anodic redox chemistry of the ferrocene-decorated $[^{Fc}DIP^{H}P][I_3]$ has been described.[17] In that report, both ligand and phosphorus centred oxidation events could be discerned by comparison of cyclic voltammograms of $[^{Fc}DIP^{H}P][I_3]$, $[^{dipp}DIP^{H}P][I_3]$ and the proligand $^{Fc}DIP^{H}$.

Given the widespread utility of DIP ligand-based electron storage (reduction) in transition metal bond activation and catalysis[26] and the increasingly successful exploitation of main-group element redox cycling[27-31] in expanding the (catalytic) chemistry of select main-group complexes to rival that of the transition metals,[32] we decided to examine in more depth the redox behavior of some DIP complexes of phosphorus. In particular, we herein describe a pair of cationic phosphorus complexes featuring P(I) and P(III) centres supported by a DIP ligand bearing *t*Bu substituents at its imine carbons. Despite report of the synthesis of this sterically bulky DIP ligand appearing over a decade ago,[33] its coordination chemistry has yet to be described beyond *in silico* modeling.[34] In addition to solution and solid-state structural characterization, we also use electrochemical analysis

to demonstrate that the P(I) complex can undergo reversible one-electron reduction, suggesting the DIP ligand can retain its redox activity in main-group complexes.

RESULTS AND DISCUSSION

As noted above, combining phosphorus(III) halides PX_3 (X = Br, I) with multidentate ligands can enable formation of P(I) complexes upon elimination of X_2,[35,36] a route also demonstrated for heavier chalcogen salts.[37] The liberated X_2 is typically either trapped by an appropriate halogen acceptor (e.g., cyclohexene for Br_2) or incorporated into the anion (e.g., formation of I_3^-).[23] Building on observations that tautomerization of Me-substituted DIP ligands can complicate their reactivity with main group centres,[16] we pursued a DIP variant with tertiary substitution at its α-carbons. In addition to adding electron-releasing substituents that may help stabilize a higher valent P(III) analog, the chosen DIP scaffold with *tert*-butyl substituents presents the added benefit of increased solubility in common organic solvents,[33] and as noted above, its coordination chemistry has yet to be described.

Synthesis of the proligand $^{dipp}DIP^{tBu}$ was accomplished by step-wise installation of the two imine arms by lithiation of 2,6-dibromopyridine with *n*BuLi and addition of *N*-(dipp) *tert*-butyl imidoyl chloride[38] [dipp = (2,6-diisopropyl)phenyl] in CH_2Cl_2/THF (Scheme 1), following the procedure reported for a closely related analog $^{Ar}DIP^{tBu}$ [Ar = (2,6-dimethyl)phenyl].[33] The $^{dipp}DIP^{tBu}$ proligand was isolated in essentially quantitative yield (~99 % yield) as a colorless powder following washing with CH_3CN. Multinuclear NMR spectroscopic analysis confirmed production of the C_{2v} symmetric free ligand, with seven distinct signals observable by ^1H NMR: a set of overlapping doublets and a septet for magnetically equivalent *i*Pr substituents, as well as a

doublet and triplet in the aromatic region, corresponding to the flanking aryl substituents, a singlet for the *t*Bu groups on the imine, and one doublet and triplet for the central pyridine moiety.

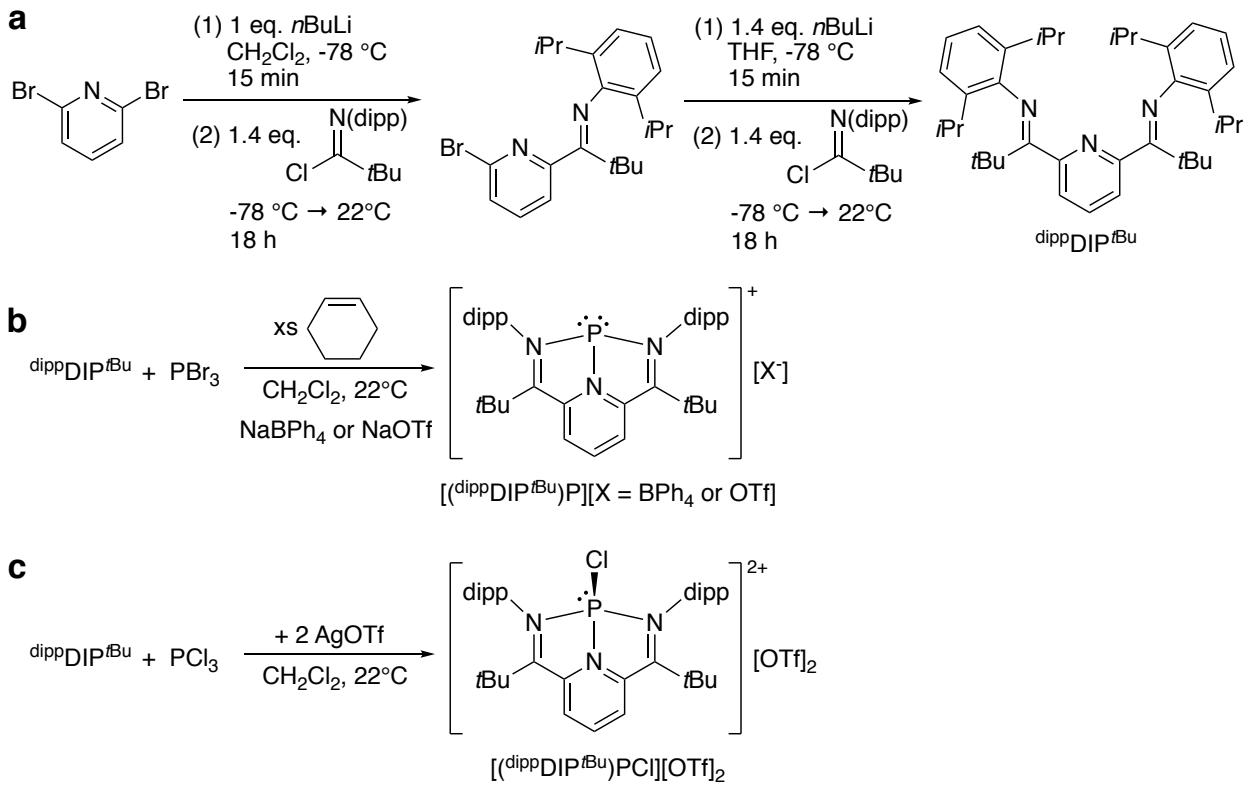

Scheme 1. Synthesis of $^{dipp}DIP^{tBu}$ and its phosphorus complexes.

Addition of PBr_3 to a CH_2Cl_2 solution of $^{dipp}DIP^{tBu}$ in the presence of a six-fold molar excess of cyclohexene at room temperature produced a yellow solution that changed to red over the course of two hours, in line with previously reported (DIP)P(I) complexes.[16] To minimize dynamic behavior between bound and unbound halides in the oxidized species (*vide infra*), the bromide counterion was then replaced with a weakly-coordinating anion by addition of either one equivalent of $NaBPh_4$ in CH_3CN or AgOTf (OTf = OSO_2CF_3; trifluoromethanesulfonate) in CH_2Cl_2. Salt metathesis was accompanied by the appearance of resonances diagnostic of the anion

in the respective ^{1}H NMR (BPh_4) or $^{19}F\{^{1}H\}$ NMR (OTf) spectra. Direct addition of the metathesis reagent at the outset of the reaction does not appear to affect the course of the reaction and conversion to the P(I) complexes is unimpeded.

Upon complexation, there is a marked change in the chemical shifts of the *meta* and *para* hydrogen nuclei of the DIP pyridine due to coordination to a cationic phosphorus centre.[16,18,20] Comparing the two salts, these signals are more shielded in [(^{dipp}DIP$^{t\text{Bu}}$)P][BPh_4] than in [(^{dipp}DIP$^{t\text{Bu}}$)P][OTf], consistent with greater inter-ion separation for the bulkier borate counterion. Overall, the ^{1}H NMR spectra of both salts indicate a C_{2v}-symmetric structure in solution, with magnetically equivalent *i*Pr substituents and similar $^{31}P\{^{1}H\}$ chemical shifts ([(^{dipp}DIP$^{t\text{Bu}}$)P][BPh_4]: δ_P = 149.9 ppm; [(^{dipp}DIP$^{t\text{Bu}}$)P][OTf]: δ_P = 149.7 ppm). Interestingly, both red solids appear to be stable in air. ^{1}H and $^{31}P\{^{1}H\}$ NMR spectroscopy show no evidence of hydrolysis or oxidation after two weeks in ambient atmosphere. Crystals of [(^{dipp}DIP$^{t\text{Bu}}$)P][BPh_4] suitable for X-ray diffraction were obtained by layering a saturated CH_2Cl_2 solution with pentane at room temperature overnight and used to confirm the molecular structure (Figure 2a).

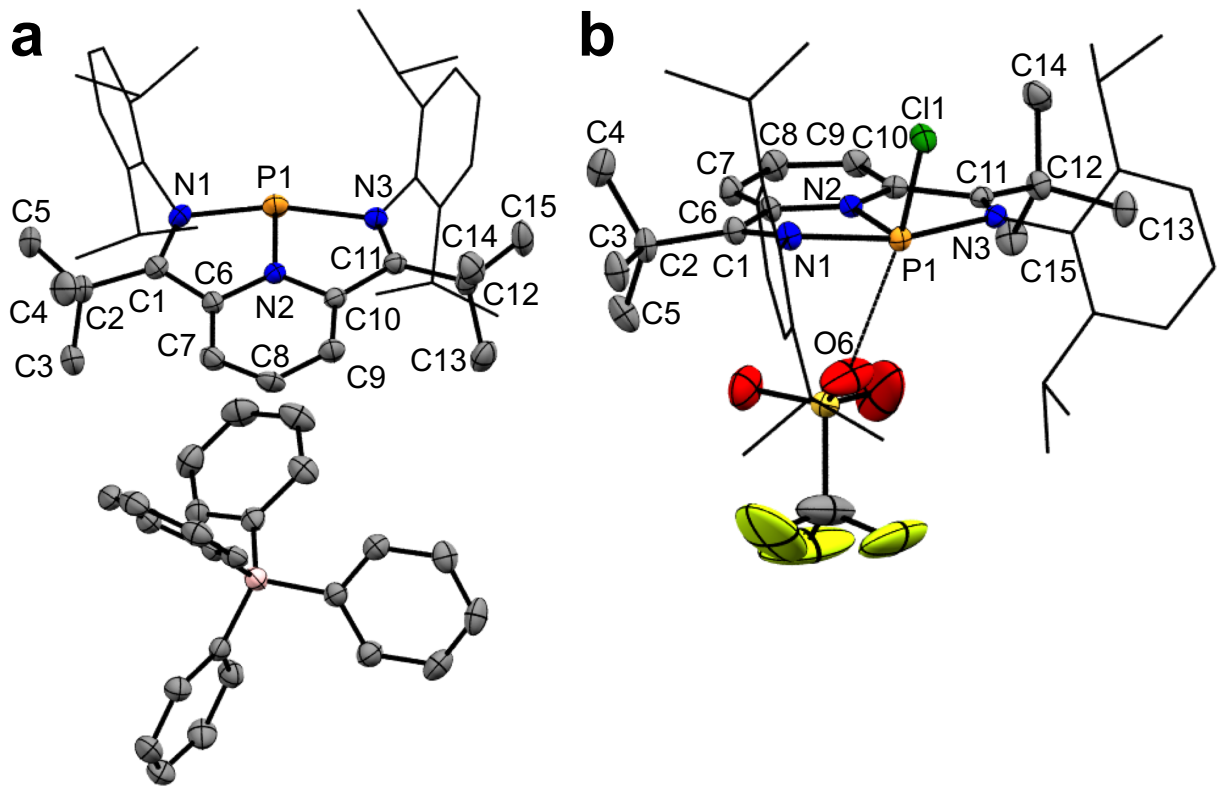

Figure 2. Molecular structures of (a) [(^{dipp}DIP^{tBu})P][BPh_4] and (b) [(^{dipp}DIP^{tBu})PCl][$OTf]_2$ with thermal displacement parameters depicted at 50 % probability levels. Hydrogen atoms, select atom labels and the second triflate counterion (b) omitted for clarity. Selected bond distance (Å) and angles (°): [(^{dipp}DIP^{tBu})P][BPh_4] N1-P1 1.8933(19), N2-P1 1.7111(17), N3-P1 2.0055(18), C1-N1 1.318(3), C11-N3 1.309(3), H_{anion}---$H_{para,pyr}$ 2.513; N1-P1-N3 162.75(8), N1-P1-N2 81.26(8), N2-P1-N3 80.49(8). [(^{dipp}DIP^{tBu})PCl][$OTf]_2$ N1-P1 1.9989(19), N3-P1 1.7752(18), N3-P1 2.0009(19), P1-Cl1 2.0192(8) Å, C1-N1: 1.285(3), C11-N3 1.294(3) P---O6 2.980; N1-P1-N3 161.47(8), N1-P1-N2 81.36(8), N2-P1-N3 81.66(8), N1-P1-Cl1 88.77(6), N2-P1-Cl1 105.59(7), N3-P1-Cl1 88.36(6).

Coordination of the imine nitrogen donors to P occurs asymmetrically in the solid-state [N1-P1 1.8933(19) Å, N3-P1 2.0055(17) Å]. Both this asymmetry and the two P-N distances lie within

the range of those previously reported.[16,17] The solid-state asymmetry contrasts the symmetric coordination environment observed in solution, again consistent with literature (DIP)P(I) complexes, as is the closer bonding distance to the pyridine nitrogen [N2-P1 1.7111(17) Å] compared to the imine arms. DFT optimization of the ground-state structure of $[(^{dipp}DIP^{tBu})P]^+$ (M06/def2SVP level of theory; SMD: CH_2Cl_2) reproduces this asymmetry, with calculated N1-P1 and N3-P1 distances of 1.848 Å and 2.050 Å respectively (see Supporting Information, Table S3). The imine C=N distances are significantly longer [C1-N1 1.318(3) Å, C11-N3 1.309(3) Å] compared to the structure of a related proligand $^{Ar}DIP^{tBu}$ (Ar = 2,6-dimethylphenyl; average d(C=N) = 1.27 Å],[33] consistent with iminium and pyridinium charge delocalization character upon coordination to phosphorus. Hemilability of donor arms in phosphorus coordination complexes has been exploited to access masked Lewis acidic character for P(III) dications[18,21] and diimine-ligated phosphinidenes.[39] The P(I) centre has *pseudo*-T-shaped geometry, with a tied-back N1-P1-N3 angle of 162.75(8)° (DFT: 162.4°) and two lone pairs. The DIP ligand remains planar, with a negligible deviation [1.8(3)°] of the imine nitrogen atoms from the plane of the pyridine ring. The diisopropyl groups are nearly orthogonal to the plane of the ligand [89.1(3), 79.8(3)°] forming a steric pocket around the phosphorus centre, similar to what is observed with α-diimine ligand-metal complexes.[40] A somewhat close H---H distance between the *para*-H on the pyridine ring and *ortho*-proton on the BPh_4 moiety mirrors the interaction in solution indicated by the shielded ^1H NMR spectrum.

With a P(I) complex in hand, we turned our attention towards a P(III) variant. Thus far, only two (DIP)P(III) complex have been reported in the literature, with a phenyl substituent installed at the phosphorus to limit reactivity.[18] As aforementioned, P(I) and P(III) centres supported by the same ligand have not been described, precluding precise comparison of the ligand environment in a pair

of redox-related molecules. Combining a CH_2Cl_2 solution of PCl_3 and a light-yellow mixture of $^{dipp}DIP^{tBu}$ with two equivalents of AgOTf in the same solvent immediately produced an orange-red solution with precipitation of AgCl. The reaction was shown to be complete after 1 h, with conversion to a new single product peak in the $^{31}P\{^1H\}$ NMR spectrum (δ = 52.0 ppm) and complete consumption of PCl_3 (δ = 220 ppm). An orange solid was obtained in 81 % yield following filtration and precipitation by addition of pentane. The ^1H NMR spectrum revealed a single DIP-containing environment for $[(^{dipp}DIP^{tBu})PCl][OTf]_2$. Complexation to a P-Cl moiety produces a C_s-symmetric structure, with inequivalent methine protons of the *iso*propyl groups on the dipp substituents above and below the plane of the central DIP framework. Compared to the free ligand, shifts in the resonances assigned to the 3- and 4-position of the pyridine ring are deshielded more so than in $[(^{dipp}DIP^{tBu})P[X]$ (X = BPh_4, OTf), consistent with coordination to a more cationic phosphorus centre. This correlates well with the emerging trend that decreased electron density at the ligated element centre results in a more deshielded H_{para} and H_{meta} on the pyridine ring. In comparison, increased electron density at the central atom results in an opposite shielding effect in DIP complexes of Ge(0)[14] and Sn(0)[41]. The introduction of higher cationic charge at the P(III) centre results in a lower energy non-bonding electron pair, which as such is not as delocalized into the pyridine moiety. Instead, the build-up of positive charge at the phosphorus centre inductively withdraws electron density from the pyridine ring and contributes to the H_{para} and H_{meta} deshielding. $[(^{dipp}DIP^{tBu})PCl][OTf]_2$ is stable under inert atmosphere for upwards of three months but decomposes overnight on exposure of the solid compound to ambient atmosphere.

Crystals suitable for X-ray analysis (Figure 2b) were obtained by layering *n*-pentane over a concentrated CH_2Cl_2 solution with a few added drops of CH_3CN to fully solubilize the complex

and storing at -30 °C. The crystal structure of the P(III) complex includes two triflate counter-ions, one of which was modelled successfully. The second triflate exhibited disorder and was best modelled over two positions, using appropriate constraints and restraints. In contrast to the P(I) structure, coordination of the imine nitrogen donors is symmetric, with statistically indistinguishable N1-P1 [2.0009(19) Å] and N3-P1 [1.9989(19) Å] distances. The pyridine N2-P1 distance is again shorter at 1.7752(18) Å, similar to in the two reported (DIP)P(III)Ph salts.[18] This distance is longer than in the P(I) complex, despite the increase in positive charge, ascribable to the increased coordination number of the P(III) centre. The ligand environment is close to planar around phosphorus [N1-P1-N3 161.47(8)°] while the dipp *i*Pr substituents on N1 and N3 are again twisted out of the plane at angles of 73.5° and 73.2°. The imine C=N bonds are noticeably shorter [C1-N1 1.285(3) Å, C11-N3 1.294(3) Å] than the corresponding distances in the P(I) complex [C1-N1 1.318(3) Å, C11-N3 1.309(3) Å]. This would be expected if electron density from the P(I) centre that delocalizes into C=N π* orbitals in the reduced congener is absent in the higher oxidation state P(III) complex. The P1-Cl1 distance at 2.0192(8) Å is significantly shorter than the sum of the P-Cl covalent radii (Σ_{CR} = 2.10 Å)[42] with the increased cationic charge of the P(III) centre causing contraction of the P-Cl bond. As is the case in [(^{dipp}DIP^{t}Bu)P]$^{+}$, the DFT-optimized structure of the dication reproduces the solid-state geometrical parameters, with essentially symmetrical ligand coordination (N1-P1 2.007 Å, N3-P1 1.997 Å), as well as shortened P-Cl bond (P1-Cl1 2.044 Å) and C=N bonds (C1-N1 1.285 Å, C11-N3 1.285 Å). In the solid-state, close contact of one triflate counterion is observed with a P---O contact distance of 2.980 Å, while the second triflate is well outside of the sum of the van der Waals radii (2.32 Å).[43]

In solution, the P(I) complex appears red and the P(III) more orange in color. UV-Vis absorption spectra in CH_2Cl_2 accordingly contain a broad, low energy band (Figure 3a), with

[(^{dipp}DIP^{tBu})P][BPh$_4$] absorbing considerably more strongly at longer wavelengths (λ_{max} = 517 nm, ε = 4990 M^{-1} cm^{-1}) than [(^{dipp}DIP^{tBu})PCl][OTf]$_2$ (λ_{max} = 490 nm, 182 M^{-1} cm^{-1}). Higher energy bands (300-400 nm) attributable to ligand π-π* transitions are also evident, with a small bathochromic shift (20 nm) in these band maxima for the P(I) complex mirroring the red shift in the λ_{max}. DFT analysis indicates the P(I) centre bears a significant portion of the HOMO in the form of a *p*-type orbital containing a primarily non-bonding lone pair (Figure 4; see SI for expanded MO diagrams). The LUMO is localized largely on the pyridine ring with C=N π* contributions. The frontier orbitals in general are quite similar to those previously calculated for analogs [(^{H}DIP^{Me})P]$^+$ and [(^{H}DIP^{Me})As]$^+$, where aryl substituents were replaced with hydrogens for computational simplicity.[44]

In contrast, the HOMO-1 and HOMO of the P(III) complex are localized in the π-system of the DIP imine arms. The LUMO is pyridine-based, with a significant portion lying on the *para* carbon corroborating its deshielded ^{1}H NMR chemical shift, and also features P-Cl σ* character. The lowest energy absorption for the P(I) complex is accurately reproduced by time-dependent DFT (TD-DFT) and has largely HOMO→LUMO character. An electron-hole difference map showing the charge transfer involved in this transition is shown in Figure 3b. DFT predicts a larger HOMO-LUMO gap for the P(III) cation, however the lowest energy transition with a significant oscillator strength predicted by TD-DFT involves charge transfer from the HOMO-3→LUMO (electron-hole map, Figure 3c).

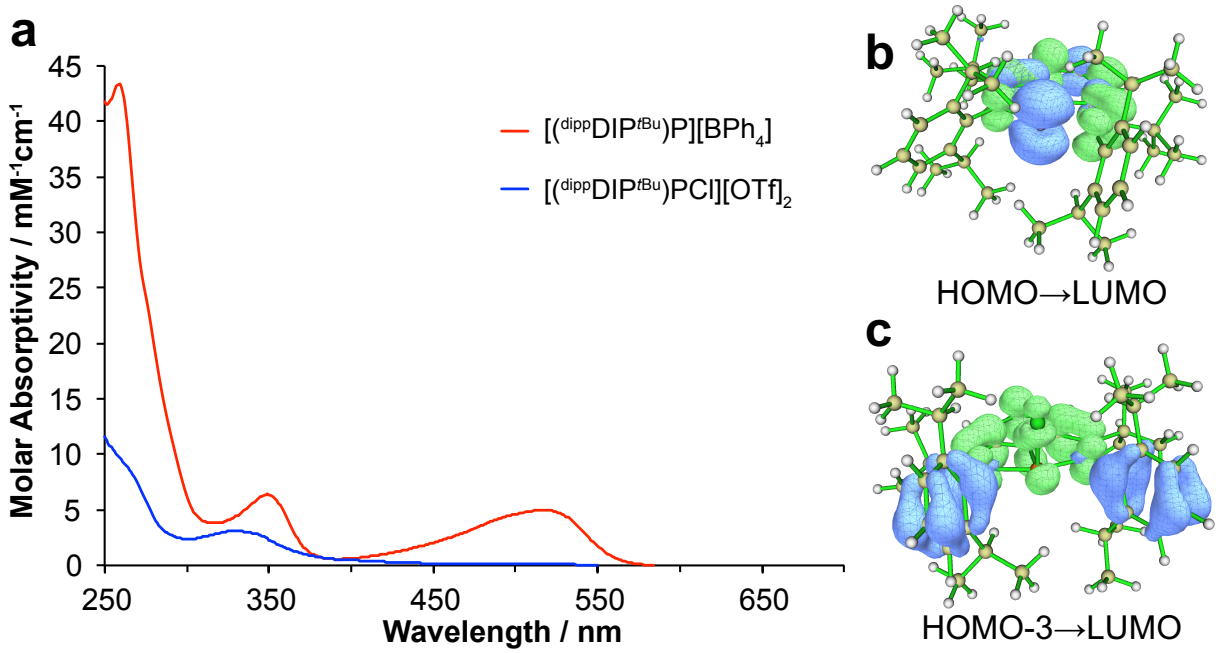

Figure 3. (a) UV-Vis absorption spectra of [(^{dipp}DIP^{t}Bu)P][BPh_4] and [(^{dipp}DIP^{t}Bu)PCl][$OTf]_2$ in CH_2Cl_2; TD-DFT difference maps [M06/def2SVP] in CH_2Cl_2 showing electron density gain (green) and depletion (blue) distribution maps (isosurface = 0.003) illustrating the charge transfer character of the lowest energy transition for (b) [(^{dipp}DIP^{t}Bu)P][BPh_4]: HOMO→LUMO and (c) [(^{dipp}DIP^{t}Bu)PCl][$OTf]_2$: HOMO-3→LUMO.

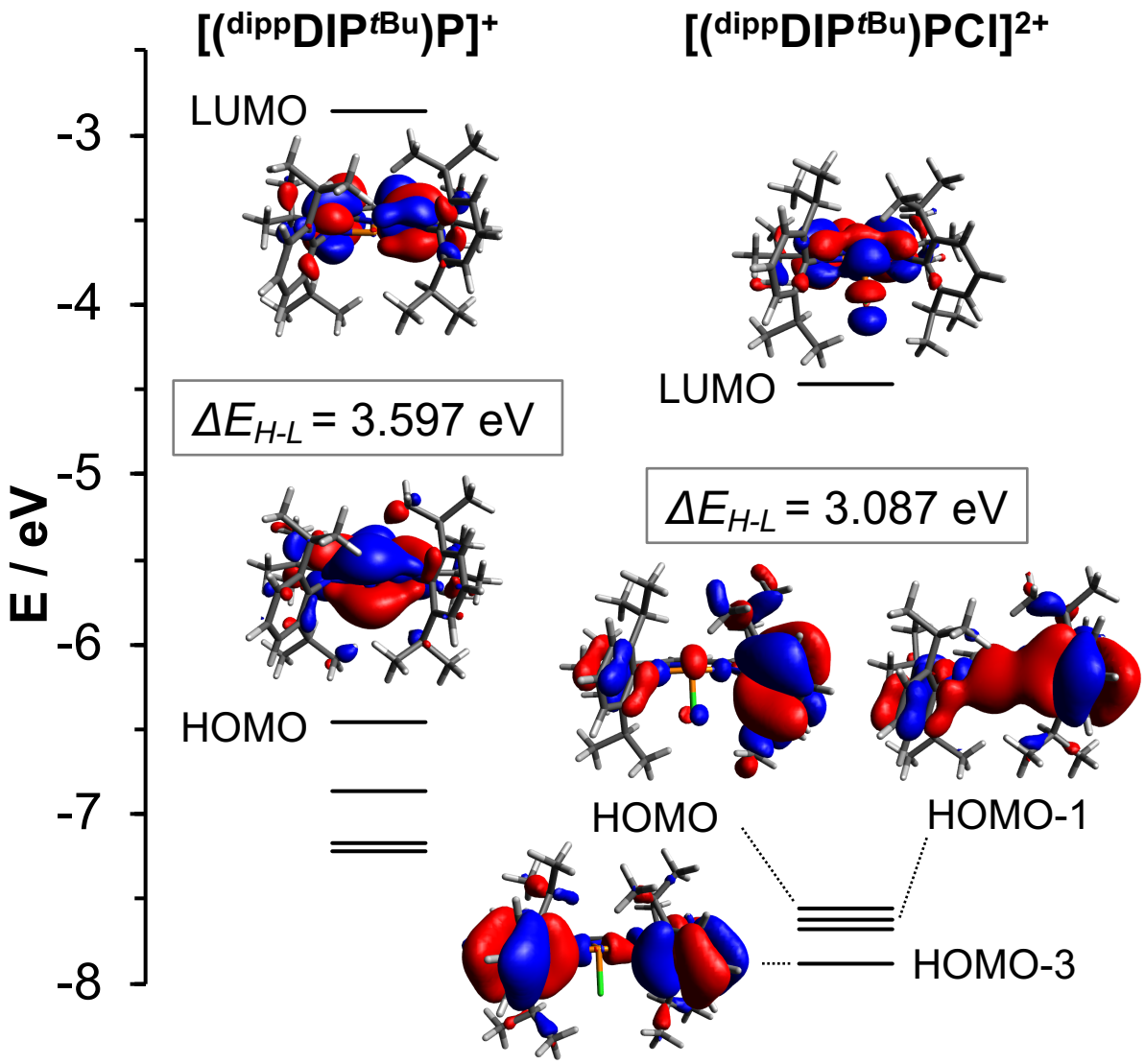

Figure 4. DFT optimized molecular orbital energy level diagrams and selected orbital isosurfaces (SMD-M06/def2SVP, CH_2Cl_2 solvent field) of $[(^{dipp}DIP^{tBu})P]^+$ (left) and $[(^{dipp}DIP^{tBu})PCl]^{2+}$ (right).

The rest of the lowest energy manifold of $[(^{dipp}DIP^{tBu})P]^+$ is similarly attributed by TD-DFT to charge-transfer (CT) type transitions in which electron density is relocated from the P(I) lone pairs (HOMO, HOMO-1) to π^*-type orbitals on the DIP ligand (LUMO). Higher energy transitions are

dominated by intraligand charge-transfer, with the flanking aryl rings (HOMO-2, HOMO-3) acting as donor sites. For $[(^{dipp}DIP^{tBu})PCl]^{2+}$, the significantly weaker lower energy band accordingly has much smaller oscillator strengths predicted by TD-DFT. This band is ascribed primarily to a transition involving intraligand CT from the flanking aryl rings (HOMO-3), with a small contribution from phosphorus-based electron density (HOMO-2), to pyridine-based π^*-type acceptor MOs which also exhibit some P-Cl σ^* character (LUMO, LUMO+1).

As befits the ability to isolate both P(I) and P(III) congeners, (irreversible) oxidation of $[(^{dipp}DIP^{tBu})P][BPh_4]$ is observed electrochemically at ~ +0.4 V vs $FcH^{0/+}$ (FcH = ferrocene; Figure 5). Interestingly, the complex also shows a reversible reduction at -1.38 V. This cathodic event is consistent with ligand-based reduction, common for diiminepyridine complexes of metals.[45,46] However, one could also postulate the reduction as forming a formally neutral P(0) complex. The preparation of reduced, low-valent main group-DIP species has been examined previously with germanium[14] and tin[41]. These heavier main-group elements possess significantly more metal character than phosphorus, and as such, can accommodate electrons in lower energy orbitals, *vis-à-vis* the inert-pair effect. The increased s-character on the metal precludes the greater contributions from the triplet state, as shown by DFT calculations for the (DIP)Ge complex,[14] while in the case of phosphorus, one-electron reduction to a formal "P(0)" would form a radical. Attempts to isolate a chemically reduced species have thus far not yielded an isolable complex.

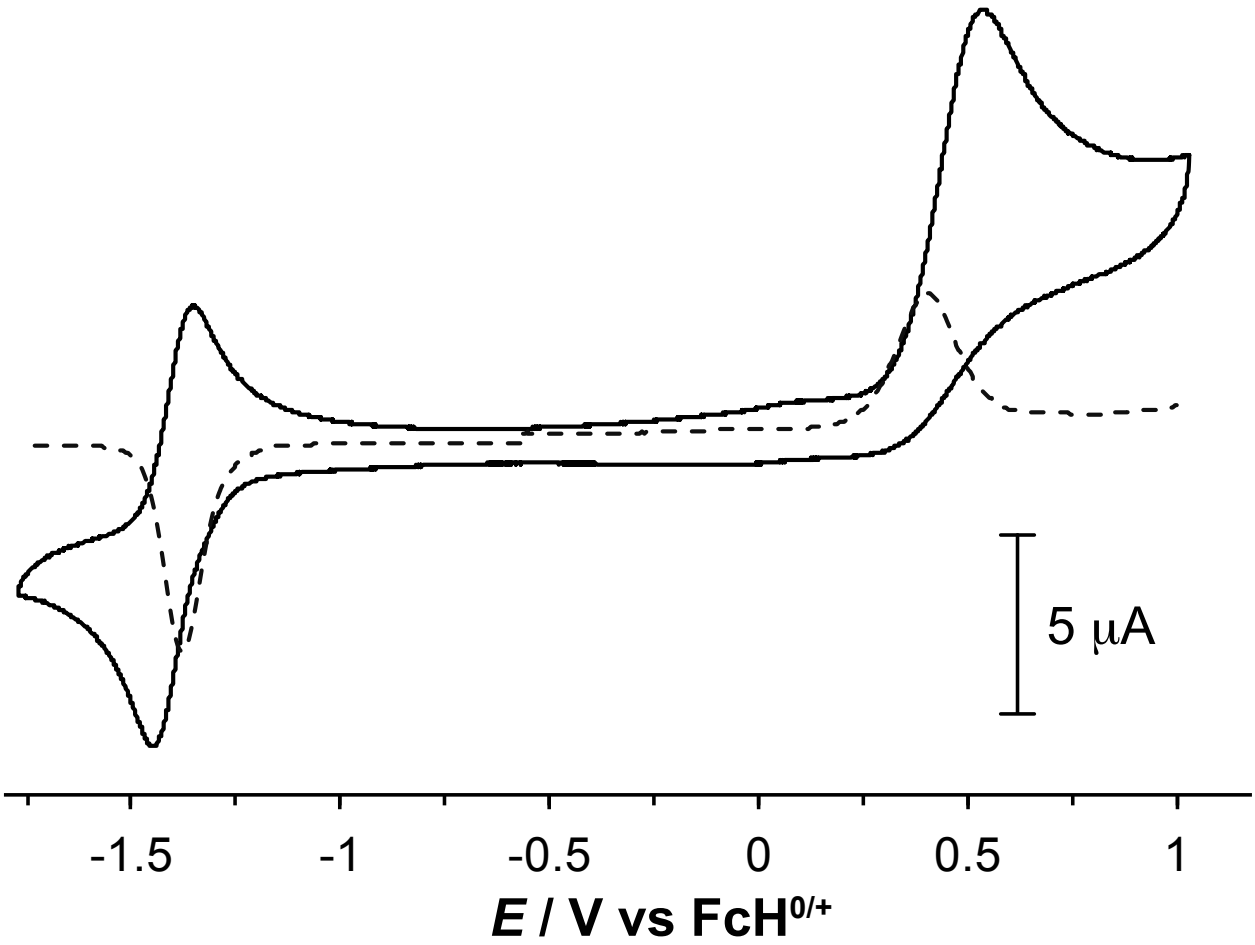

Figure 5. CV (—) and DPV (---) of [(^{dipp}DIP^{tBu})P][BPh_4] ([analyte] = 1.0 mM, 0.1 M nBu$_4$PF_6, CH_2Cl_2, glassy carbon working electrode, ν = 100 mV s^{-1}).

In conclusion, a pair of cationic (^{dipp}DIP^{tBu})P(I) and (^{dipp}DIP^{tBu})P(III) complexes has been isolated and characterized, with the main group centre supported in each case by the same DIP ligand framework, enabling direct examination of differences in the ligand environment that arise from coordination to a pnictogen in different oxidation states. This includes only the third reported example of a (DIP)P(III) complex and first with a halide substituent.[24] In addition, the reported complexes represent the first examples of coordination of a DIP ligand bearing sterically imposing *t*Bu substituents at the imine carbons. While this position is relatively remote from the site of

ligation, previous attempts at metalation with both ferric and ferrous iron were reported to be unsuccessful[33] despite computational modeling suggesting coordination to late transition metals should produce stable complexes.[34] Finally, the pair of complexes exhibit interesting electronic structures, with both "P to ligand" and intraligand CT character observed by UV-Vis absorption spectroscopy, as elucidated by TD-DFT. Electrochemical analysis reveals an electrochemically reversible reduction for the P(I) complex [(^{dipp}DIP^{tBu})P][BPh_4], suggesting isolation of a reduced "P(0)" DIP complex may be feasible. Efforts to do so are currently underway.

EXPERIMENTAL SECTION

Unless otherwise specified, all air sensitive manipulations were carried out either in a N_2-filled glove box or using standard Schlenk techniques under Ar. *N*-(2,6-diisopropyl-phenyl)-2,2-dimethyl-propionimidoyl chloride was prepared according to a literature procedure.[38] PCl_3 and PBr_3 (Sigma Aldrich) were purified by vacuum distillation prior to use. AgOTf (Alfa Aesar), $NaBPh_4$ (Sigma Aldrich), and nBu$_4$NPF$_6$ (electrochemical grade, Sigma Aldrich) were purchased and used without further purification. Organic solvents were dried and distilled using appropriate drying agents prior to use. NMR spectra were recorded on Bruker Avance 300 MHz or Bruker Avance-III 500 MHz spectrometers. ^{1}H and ^{13}C{^{1}H} NMR spectra were referenced to residual solvent peaks, while ^{31}P{^{1}H} (85% H_3PO_4 = 0 ppm) and ^{19}F{^{1}H} ($CFCl_3$ = 0 ppm) spectra were referenced to external standards. Electronic absorption spectra were recorded on an Agilent Technologies Cary 5000 Series UV-Vis-NIR spectrophotometer in dual beam mode (range: 230–1600 nm). High-resolution mass spectra were recorded using a Bruker microOTOF-QIII. Cyclic voltammetry was carried out using a CH Instruments 760C Series electrochemical analyzer/workstation in conjunction with a three-electrode cell. A BASi glassy carbon disk

electrode (3.0 mm diameter) was used as the working electrode, a platinum-wire counter electrode, with a non-aqueous Ag/Ag^+ quasi-reference electrode separated from the solution by a porous Teflon tip. All cyclic voltammetry (CV) and differential pulse voltammetry (DPV) measurements were conducted with 0.1 M nBu$_4$NPF$_6$ as the supporting electrolyte, at scan rates ranging from 100 mV/s to 500 mV/s. Ferrocene (FcH) was added to each solution as an internal reference, allowing the potentials to be referenced to the $FcH^{0/+}$ redox couple. Crystallographic data for the structures in this paper have been deposited with the Cambridge Crystallographic Data Centre, under CCDC deposition numbers 1981660 ([(^{dipp}DIP^{t}Bu)P][BPh$_4$]) and 1981661 ([(^{dipp}DIP^{t}Bu)PCl][OTf]$_2$). The data can be obtained free of charge from The Cambridge Crystallographic Data Centre via www.ccdc.cam.ac.uk/structures.

Synthesis of [1-(6-bromo-pyridin-2-yl)-2,2-dimethyl-propylidene]-(2,6-diisopropyl-phenyl)amine: Prepared according to the procedure reported by Zubris and coworkers for the analogous reaction using *N*-(2,6-diisopropyl-phenyl)-2,2-dimethyl-propionimidoyl chloride.[33] A 100 mL Schlenk flask was charged with the 2,6-dibromopyridine (1.80 g, 7.60 mmol, 1.0 equiv.) and 30 mL of CH_2Cl_2. The mixture was subsequently cooled to -78 °C in a dry ice-acetone bath, following which a 1.6 M solution of *n*BuLi in hexanes (4.75 mL, 7.60 mmol, 1.0 equiv.) was added and the yellow solution was stirred at this temperature for 20 min. A solution of the imidoyl chloride (2.98 g, 10.64 mmol, 1.4 equiv.) in CH_2Cl_2 was subsequently added dropwise over the course of 15 min. The reaction was stirred for an additional 30 min at -78 °C, then allowed to warm to room temperature slowly overnight. The resulting slurry was filtered through a medium-porosity glass frit to give a light yellow filtrate. The volatiles were removed under reduced pressure and the resulting residue was dried under vacuum for 4 hours to give a viscous semi-solid. This residue

was dissolved in 2.5 % ethyl acetate-hexanes and passed through a 15 cm plug of silica. Removing the solvent and drying *in vacuo* gave the monoimine as a yellow solid (2.41 g, 79 %). ^{1}H NMR ($CDCl_3$, 300 MHz, 25 °C): δ 7.21 (m, 2H, H_{Ar}), 6.87 (m, 3H, H_{Ar}), 6.63 (m, 1H, H_{Ar}), 2.90 (sept, 2H, J_{HH} = 6.8 Hz, C*H*(CH_3)$_2$), 1.37 (s, 9H, C(CH_3)$_3$), 1.11 (d, 6H, J_{HH} = 6.8 Hz, CH(CH_3)$_2$), 1.10 ppm (d, 6H, J_{HH} = 6.8 Hz, CH(CH_3)$_2$). ^{13}C{^{1}H} NMR (CD_3CN, 75 MHz, 25 °C): δ 173.7 (*t*Bu*C*=N), 156.8 (C_{Ar}), 145.7 (C_{Ar}), 141.0 (C_{Ar}), 137.4 (C_{Ar}), 135.7 (C_{Ar}), 127.0 (C_{Ar}), 122.3 (C_{Ar}), 120.7 (C_{Ar}), 40.7 (*C*(CH_3)$_3$) 29.0 (C(*C*H_3)$_3$), 28.3 (*C*H(CH_3)$_2$), 23.7 (*C*H_3), 21.7 ppm (*C*H_3).

Synthesis of ^{dipp}DIP$^{t\mathrm{Bu}}$: Prepared using a modified literature procedure reported by Zubris and coworkers.[33] A 100 mL Schlenk flask was charged with [1-(6-bromo-pyridin-2-yl)-2,2-dimethyl-propylidene]-(2,6-diisopropyl-phenyl)amine (0.50 g, 1.25 mmol, 1.0 equiv.) and anhydrous THF (20 mL) and subsequently cooled to -78 °C in a dry ice-acetone bath. A 1.6 M solution of *n*BuLi in hexanes (1.09 mL, 1.74 mmol, 1.4 equiv.) was then added dropwise over 15 min. The resulting yellow/brown mixture was stirred for 20 min before adding a solution of the imidoyl chloride (0.49 g, 1.74 mmol, 1.4 equiv.) in 10 mL of anhydrous THF, giving an orange/brown mixture. The reaction was stirred for an additional 30 min at -78 °C, then allowed to warm to room temperature slowly overnight. The solvent was then removed *in vacuo* to give an oily solid, to which 40 mL of CH_3CN was added. This mixture was isolated via vacuum filtration, yielding a colorless solid (0.70 g, 99 %). ^{1}H NMR ($CDCl_3$, 300 MHz, 25 °C): δ 7.17 (t, 1H, J_{HH} = 7.9 Hz, PyrH_p), 6.88 (d, 4H, J_{HH} = 7.9 Hz, ArH_m), 6.81 (t, 2H, J_{HH} = 7.8 Hz ArH_p), 6.65 (d, 2H, J_{HH} = 7.9 Hz PyrH_m), 2.82 (sept, 4H, J_{HH} = 6.5 Hz, C*H*(CH_3)$_2$), 1.24 (s, 18H, C(CH_3)$_3$), 1.11 ppm (m (overlapping signals), 24H, CH(CH_3)$_2$). ^{13}C{^{1}H} NMR (CD_3CN, 75 MHz, 25 °C): δ 173.6 (*t*Bu*C*=N), 155.0 (C_{Ar}), 146.2 (C_{Ar}), 134.8 (C_{Ar}), 134.1 (C_{Ar}), 122.6 (C_{Ar}), 122.2 (C_{Ar}), 121.4 (C_{Ar}), 40.8 (*C*(CH_3)$_3$) 29.1

(C(CH_3)$_3$), 28.4 (CH(CH$_3$)$_2$), 23.3 (CH_3), 21.5 ppm (CH_3). HRMS $C_{39}H_{55}N_3$ calcd (found): 566.4469 (566.4488).

Synthesis of [(^{dipp}DIP^{t}^{Bu})P][OTf]: A 20 mL glass scintillation vial was charged 5 mL of CH_2Cl_2, ^{dipp}DIP^{t}^{Bu} (141.5 mg, 0.25 mmol, 1.0 equiv.) and cyclohexene (123.2 mg, 1.5 mmol, 151 µL, 6.0 equiv.). PBr_3 (67.7 mg, 0.25 mmol, 23.8 µL, 1.0 equiv.) was then added, producing a red solution. The mixture was stirred for 30 min at room temperature. Solid AgOTf (64.3 mg, 0.25 mmol, 1 equiv.) was then added immediately forming a colorless precipitate of AgCl. The mixture was stirred for 30 min and the dark red solution isolated by filtration. The volatiles were removed *in vacuo* to give a dark red solid. Recrystallization from CH_2Cl_2 gave (^{dipp}DIP^{t}^{Bu})P[OTf] as dark red crystals, which were washed twice with 2 mL of Et_2O and dried *in vacuo*. Crude yield: 0.147 g (79 %); Crystalline recovery: 0.084 g (56 % recovery). ^{1}H NMR (CD_2Cl_2, 500 MHz, 25 °C): δ 9.32 (d, 2H, J_{HH} = 8.3 Hz, PyrH_m), 8.34 (t, 1H, J_{HH} = 8.3 Hz, PyrH_p), 7.40 (t, 2H, J_{HH} = 7.7 Hz, ArH_p), 7.24 (d, 4H, J_{HH} = 7.7 Hz, ArH_m), 2.32 (sept, 4H, J_{HH} = 6.7 Hz, CH(CH$_3$)$_2$), 1.58 (s, 18H, C(CH_3)$_3$), 1.22 (d, 12H, J_{HH} = 6.7 Hz, CH(CH_3)$_2$), 1.02 ppm (d, 12H, J_{HH} = 6.7 Hz, CH(CH_3)$_2$). ^{13}C{^{1}H} NMR (CD_2Cl_2, 125 MHz, 25 °C): δ 164.1 (d, J_{CP} = 6.2 Hz, tBuC=N), 143.4 (d, J_{CP} = 1.8z Hz, C_{Ar}), 136.8 (d, J_{CP} = 7.3 Hz, C_{Ar}), 134.4 (d, J_{CP} = 6.3 Hz, C_{Ar}), 131.3 (d, J_{CP} = 3.5 Hz, C_{Ar}), 129.8 (C_{Ar}), 125.7 (d, J_{CP} = 4.6 Hz, C_{Ar}), 124.2 (C_{Ar}) 41.0 (d, J_{CP} = 3.7 Hz, C(CH$_3$)$_3$) 32.7 (C(CH$_3$)$_3$), 29.2 (d, J_{CP} = 3.2 Hz, CH(CH$_3$)$_2$), 27.2 (d, J_{CP} = 3.6 Hz, CH(CH$_3$)$_2$), 23.6 ppm (CH_3). ^{31}P{^{1}H} NMR (CD_2Cl_2, 202 MHz, 25 °C): δ 149.7 ppm (s). ^{19}F NMR (CD_2Cl_2, 471 MHz, 25 °C): δ -78.9 ppm (s, $SO_3C$$F_3$). HRMS $C_{39}H_{55}N_3$ calcd (found): 596.4128 (596.4084).

Synthesis of [(^{dipp}DIP^{tBu})P][BPh$_4$]: A 20 mL glass scintillation vial was charged 5 mL of CH_2Cl_2 with ^{dipp}DIP^{tBu} (0.142 g, 0.250 mmol, 1.0 equiv.) and cyclohexene (0.123 g, 1.50 mmol, 151 µL, 6.0 equiv.). PBr_3 (0.068 g, 0.25 mmol, 23.8 µL, 1.0 equiv.) was added, resulting in the formation of a red solution. The mixture was stirred for 30 minutes at room temperature. To this solution was added $NaBPh_4$ (85.6 mg, 0.25 mmol, 1 eq) along with 1 mL of CH_3CN, resulting in the formation of colorless NaCl precipitate. The volatiles were removed *in vacuo* to give a red solid. The solid was redissolved in 3mL of CH_2Cl_2 and filtered again to give a dark red solution. The volatiles were removed *in vacuo* giving a dark red crystalline material. X-ray quality crystals were obtained by cooling a saturated CH_2Cl_2 solution in a -35 °C freezer overnight, giving [(^{dipp}DIP^{tBu})P][BPh$_4$] as dark red crystals. Crystals not selected for X-ray analysis were washed twice with 2mL of Et_2O and dried *in vacuo*. Crude yield: 0.187 g (82 %); Crystalline recovery: 0.092 g (49 % recovery). ^{1}H NMR (CD_2Cl_2, 500 MHz, 25 °C): δ 8.96 (d, 2H, J_{HH} = 8.4 Hz, PyrH_m), 7.75 (t, 1H, J_{HH} = 8.3 Hz PyrH_p), 7.41 (t, 2H, J_{HH} = 7.8 Hz, ArH_p), 7.35 (m, 8H, BPh_4), 7.24 (d, 4H, J_{HH} = 7.4 Hz, ArH_m), 7.02 (t, J_{HH} = 7.4 Hz, 8H, BPh_4), 6.87 (t, J_{HH} = 7.4 Hz, 4H, BPh_4), 2.30 (sept, 4H, J_{HH} = 6.8 Hz, CH(CH$_3$)$_2$), 1.53 (s, 18H, C(CH_3)$_3$), 1.22 (d, 12H, J_{HH} = 6.8 Hz, CH(CH_3)$_2$), 1.02 ppm (d, 12H, J_{HH} = 6.8 Hz, CH(CH_3)$_2$). ^{13}C{^{1}H} NMR (CD_2Cl_2, 125 MHz, 25 °C): δ 164.6 (q, J_{CB} = 49.3 Hz, BPh_4) 164.0 (d, J_{CP} = 3.7 Hz, tBuC=N), 143.3 (C_{Ar}), 136.5 (q, J_{CB} = 1.4 Hz, BPh_4), 134.4 (d, J_{CP} = 6.3 Hz, C_{Ar}), 130.7 (d, J_{CP} = 3.5 Hz, C_{Ar}),, 130.0 (C_{Ar}), 126.2 (q, J_{CB} = 2.7 Hz, BPh_4), 125.1 (d, J_{CP} = 4.3 Hz, C_{Ar}), 124.3 (C_{Ar}), 122.3 (BPh_4) 41.0 (dz, J_{CP} = 3.7 Hz, C(CH$_3$)$_3$) 32.7 (C(CH$_3$)$_3$), 29.2 (d, J_{CP} = 3.2 Hz, CH(CH$_3$)$_2$), 27.2 (d, J_{CP} = 3.7 Hz, CH(CH$_3$)$_2$), 22.9 ppm (CH$_3$). Note: one aromatic signal was not observed due to overlap with BPh$_4$ signals at 136.5 ppm. ^{31}P{^{1}H} NMR (CD_2Cl_2, 202 MHz, 25 °C): δ 149.9 ppm (s). HRMS $C_{39}H_{55}N_3$ calcd

(found): 596.4128 (596.4095). UV-Vis (CH_2Cl_2): λ (ε) 259 (43375 M^{-1} cm^{-1}) 349 (6400), 517 (4990).

Synthesis of [(^{dipp}DIP^{tBu})PCl][OTf]$_2$: A 20 mL glass scintillation vial was charged with ^{dipp}DIP^{tBu} (0.283 g, 0.5 mmol, 1.0 equiv), AgOTf (0.257 g, 1.0 mmol, 2 equiv.) and 5 mL of CH_2Cl_2. PCl_3 (0.069 g, 0.5 mmol, 43.7 μL) was added, resulting in the immediate formation of a dark red supernatant over a colorless precipitate. The mixture was stirred for 1 h at room temperature in the dark and then filtered to give a red solution. The volatiles were removed *in vacuo* giving an orange solid. The solid was recrystallized from CH_3CN in a -30 °C freezer to give red crystals of [(^{dipp}DIP^{tBu})PCl][OTf]$_2$, which were washed twice with 2 mL of Et_2O and 2 mL of *n*-pentane and dried *in vacuo*. Yield: 0.321 g, (69 %). ^{1}H NMR (CD_2Cl_2, 300 MHz, 25 °C): δ 9.60 (dd, 2H, J_{HH} = 8.3 Hz, J_{HP} = 2.5 Hz, PyrH_m), 9.38 (td, 1H, J_{HH} = 8.3 Hz, J_{HP} = 3.8 Hz, PyrH_p), 7.47 (m, 2H, ArH_p), 7.31 (m, 4H, ArH_m), 3.09 (sept, 4H, J_{HH} = 6.6 Hz, CH(CH_3)$_2$), 2.87 (sept, 4H, J_{HH} = 6.6 Hz, CH(CH_3)$_2$), 1.64 (s, 18H, C(CH_3)$_3$), 1.22 ppm (m (overlapping signals), 24H, CH(CH_3)$_2$). ^{31}P{^{1}H} NMR (CD_2Cl_2, 121 MHz, 25 °C): δ 52.0 ppm (s). ^{19}F NMR (CD_2Cl_2, 282 MHz, 25 °C): δ -78.7 ppm (s, SO_3CF_3). HRMS $C_{39}H_{55}N_3$ calcd (found): 596.4128 (596.4149). UV-Vis (CH_2Cl_2): λ (ε) 329 (3109 M^{-1} cm^{-1}), 490 (182).

ASSOCIATED CONTENT

Supporting Information. Extended computational plots and tables, details of computational and crystallographic analysis, NMR spectra and tables are available as supporting information. The following files are available free of charge:

Computational details, plots and tables, NMR spectra and crystallographic details (PDF)

Crystallographic Information Files for [(^{dipp}DIP^{t}Bu)P][BPh_4] and [(^{dipp}DIP^{t}Bu)PCl][$OTf]_2$ (CIF)

AUTHOR INFORMATION

Corresponding Author

*david.herbert@umanitoba.ca

Corresponding Author Homepage URL

https://home.cc.umanitoba.ca/~dherbert/

ORCIDs

Dr. Paul A. Gray: 0000-0001-6933-6002
Jason D. Braun: 0000-0002-5850-8048
Naser Rahimi: 0000-0002-8617-9122
Prof. Dr. David E. Herbert: 0000-0001-8190-2468

Author Contributions

The manuscript was written through contributions of all authors. All authors have given approval to the final version of the manuscript.

ACKNOWLEDGMENTS

We gratefully acknowledged the Natural Sciences Engineering Research Council of Canada for a Discovery Grant to DEH (RGPIN-2014-03733); the Canadian Foundation for Innovation and Research Manitoba for an award in support of an X-ray diffractometer (CFI #32146); the University of Manitoba for GETS support (JDB); and Compute Canada for access to computational resources. I.B. Lozada and P.H.M. Budzelaar are thanked for helpful discussions and for donation of chemicals (PHMB). We dedicate this paper to Prof. Neil Burford in celebration of a wonderful career, and with gratitude for his mentorship and support.

Notes

The authors declare no competing financial interest.

REFERENCES

(1) V. C. Gibson, C. Redshaw, G. A. Solan, *Chem. Rev.* **2007**, *107*, 1745-1776.

(2) Q. Knijnenburg, S. Gambarotta, P. H. M. Budzelaar, *Dalton Trans.* **2006**, 5442-5448.

(3) D. Zhu, I. Thapa, I. Korobkov, S. Gambarotta, P. H. M. Budzelaar, *Inorg. Chem.* **2011**, *50*, 9879-9887.

(4) C. Roemelt, T. Weyhermueller, K. Wieghardt, *Coord. Chem. Rev.* **2019**, *380*, 287-317.

(5) V. Lyaskovskyy, B. de Bruin, *ACS Catal.* **2012**, *2*, 270-279.

(6) Z. Flisak, W.-H. Sun, *ACS Catal.* **2015**, *5*, 4713-4724.

(7) N. Rahimi, D. E. Herbert, P. H. M. Budzelaar, *Eur. J. Inorg. Chem.* **2018**, *2018*, 4856-4866.

(8) N. Rahimi, D. E. Herbert, P. H. M. Budzelaar, *Eur. J. Inorg. Chem.* **2019**, *2019*, 780-786.

(9) S. S. Galley, S. A. Pattenaude, R. F. Higgins, C. J. Tatebe, D. A. Stanley, P. E. Fanwick, M. Zeller, E. J. Schelter, S. C. Bart, *Dalton Trans.* **2019**, *48*, 8021-8025.

(10) J. Scott, S. Gambarotta, I. Korobkov, Q. Knijnenburg, B. De Bruin, P. H. M. Budzelaar, *J. Am. Chem. Soc.* **2005**, *127*, 17204-17206.

(11) T. Jurca, J. Lummiss, T. J. Burchell, S. I. Gorelsky, D. S. Richeson, *J. Am. Chem. Soc.* **2009**, *131*, 4608-4609.

(12) T. Jurca, K. Dawson, I. Mallov, T. Burchell, G. P. A. Yap, D. S. Richeson, *Dalton Trans.* **2010**, *39*, 1266-1272.

(13) R. Pedrido, M. J. Romero, M. R. Bermejo, A. M. Gonzalez-Noya, M. Maneiro, M. J. Rodriguez, G. Zaragoza, *Dalton Trans.* **2006**, 5304-5314.

(14) T. Chu, L. Belding, A. van der Est, T. Dudding, I. Korobkov, G. I. Nikonov, *Angew. Chem., Int. Ed.* **2014**, *53*, 2711-2715.

(15) G. Reeske, A. H. Cowley, *Chem. Commun.* **2006**, 1784-1786.

(16) C. D. Martin, P. J. Ragogna, *Dalton Trans.* **2011**, *40*, 11976-11980.

(17) E. Magdzinski, P. Gobbo, C. D. Martin, M. S. Workentin, P. J. Ragogna, *Inorg. Chem.* **2012**, *51*, 8425-8432.

(18) S. S. Chitnis, J. H. W. LaFortune, H. Cummings, L. L. Liu, R. Andrews, D. W. Stephan, *Organometallics* **2018**, *37*, 4540-4544.

(19) C. D. Martin, C. M. Le, P. J. Ragogna, *J. Am. Chem. Soc.* **2009**, *131*, 15126-15127.

(20) C. D. Martin, P. J. Ragogna, *Inorg. Chem.* **2012**, *51*, 2947-2953.

(21) R. J. Andrews, S. S. Chitnis, D. W. Stephan, *Chem. Commun.* **2019**, *55*, 5599-5602.

(22) E. L. Norton, K. L. S. Szekely, J. W. Dube, P. G. Bomben, C. L. B. Macdonald, *Inorg. Chem.* **2008**, *47*, 1196-1203.

(23) B. D. Ellis, C. L. B. Macdonald, *Coord. Chem. Rev.* **2007**, *251*, 936-973.

(24) D. E. Herbert, A. D. Miller, O. V. Ozerov, *Chem. Eur. J.* **2012**, *18*, 7696-7704.

(25) G. Reeske, A. H. Cowley, *Inorg. Chem.* **2007**, *46*, 1426-1430.

(26) P. J. Chirik, K. Wieghardt, *Science* **2010**, *327*, 794-795.

(27) N. L. Dunn, M. Ha, A. T. Radosevich, *J. Am. Chem. Soc.* **2012**, *134*, 11330-11333.

(28) K. D. Reichl, N. L. Dunn, N. J. Fastuca, A. T. Radosevich, *J. Am. Chem. Soc.* **2015**, *137*, 5292-5295.

(29) W. Zhao, P. K. Yan, A. T. Radosevich, *J. Am. Chem. Soc.* **2015**, *137*, 616-619.

(30) T. V. Nykaza, T. S. Harrison, A. Ghosh, R. A. Putnik, A. T. Radosevich, *J. Am. Chem. Soc.* **2017**, *139*, 6839-6842.

(31) A. Ghosh, M. Lecomte, S.-H. Kim-Lee, A. T. Radosevich, *Angew. Chem., Int. Ed.* **2019**, *58*, 2864-2869.

(32) P. P. Power, *Nature* **2010**, *463*, 171-177.

(33) J. E. Steves, M. D. Kennedy, K. P. Chiang, W. S. Kassel, W. G. Dougherty, T. J. Dudley, D. L. Zubris, *Dalton Trans.* **2009**, 1214-1222.

(34) D. Zhu, P. H. M. Budzelaar, *Organometallics* **2008**, *27*, 2699-2705.

(35) B. D. Ellis, M. Carlesimo, C. L. B. Macdonald, *Chem. Commun.* **2003**, 1946-1947.

(36) B. D. Ellis, C. L. B. Macdonald, *Inorg. Chem.* **2006**, *45*, 6864-6874.

(37) J. L. Dutton, A. Sutrisno, R. W. Schurko, P. J. Ragogna, *Dalton Trans.* **2008**, 3470-3477.

(38) R. E. Cowley, K. P. Chiang, P. L. Holland, D. Adhikari, F. J. Zuno-Cruz, G. S. Cabrera, D. J. Mindiola, *Inorg. Synth.* **2010**, *35*, 13-19.

(39) J. Hyvl, W. Y. Yoshida, A. L. Rheingold, R. P. Hughes, M. F. Cain, *Chem. Eur. J.* **2016**, *22*, 17562-17565.

(40) I. E. Soshnikov, K. P. Bryliakov, A. A. Antonov, W.-H. Sun, E. P. Talsi, *Dalton Trans.* **2019**, *48*, 7974-7984.

(41) J. Flock, A. Suljanovic, A. Torvisco, W. Schoefberger, B. Gerke, R. Pöttgen, R. C. Fischer, M. Flock, *Chem. Eur. J.* **2013**, *19*, 15504-15517.

(42) P. Pyykkö, M. Atsumi, *Chem. Eur. J.* **2009**, *15*, 186-197.

(43) M. Mantina, A. C. Chamberlin, R. Valero, C. J. Cramer, D. G. Truhlar, *J. Phys. Chem. A* **2009**, *113*, 5806-5812.

(44) B. D. Ellis, C. L. B. Macdonald, *Inorg. Chim. Acta* **2007**, *360*, 329-344.

(45) G. M. Duarte, J. D. Braun, P. K. Giesbrecht, D. E. Herbert, *Dalton Trans.* **2017**, *46*, 16439-16445.

(46) J. D. Braun, P. A. Gray, B. K. Sidhu, D. B. Nemez, D. E. Herbert, *Dalton Trans.* **2020**, Ahead of Print – DOI: 10.1039/d0dt00543f.